P H Y S I C A L   R E V I E W   L E T T E R S

Accurate and Robust Unitary Transformations of a High-Dimensional Quantum System

B. E. Anderson,[1,2] H. Sosa-Martinez,[1] C. A. Riofrío,[3,4] Ivan H. Deutsch,[3] and Poul S. Jessen[1]

[1]*Center for Quantum Information and Control, College of Optical Sciences and Department of Physics,
University of Arizona, Tucson, Arizona 85721, USA*

[2]*National Institute of Standards and Technology and Joint Quantum Institute, NIST and the University of Maryland,
Gaithersburg, Maryland 20899, USA*

[3]*Center for Quantum Information and Control, Department of Physics and Astronomy,
University of New Mexico, Albuquerque, New Mexico 87131, USA*

[4]*Dahlem Center for Complex Quantum Systems, Freie Universität Berlin, 14195 Berlin, Germany*

Unitary transformations are the most general input-output maps available in closed quantum systems. Good control protocols have been developed for qubits, but questions remain about the use of optimal control theory to design unitary maps in high-dimensional Hilbert spaces, and about the feasibility of their robust implementation in the laboratory. Here we design and implement unitary maps in a 16-dimensional Hilbert space associated with the $6S_{1/2}$ ground state of ^{133}Cs, achieving fidelities > 0.98 with built-in robustness to static and dynamic perturbations. Our work has relevance for quantum information processing and provides a template for similar advances on other physical platforms.

Quantum control in large dimensional Hilbert spaces is an essential part of quantum information processing. For closed systems the relevant input-output maps are unitary transformations, and the fundamental challenge becomes how to implement these with high fidelity in the presence of experimental imperfections and decoherence. The goal of quantum control, then, is to find a control Hamiltonian $H_C(t)$ such that dynamical evolution over some time T accomplishes the desired transformation. For two-level systems (qubits) most aspects of this problem are well understood [1], but for systems with Hilbert space dimension $d > 2$ (qudits) questions remain regarding the design of control Hamiltonians [2] and the feasibility of robust implementation [3,4]. If the control task is simple or special symmetries are present, it is sometimes possible to find a high-performing control Hamiltonian through intuition, or to construct one using group theoretic methods [5]. A more general approach is provided by "optimal control," a well established procedure in which $H_C(t)$ is parametrized by a set of control variables, and a numerical search performed to optimize the fidelity with which the control objective is achieved [2]. The application of optimal control to quantum systems originated in nuclear magnetic resonance [1] and physical chemistry [2], and has expanded to include ultrafast physics [6], cold atoms [7,8], biomolecules [9], condensed matter spins [10], and superconducting circuits [11].

In this Letter we explore the use of optimal control to design control Hamiltonians for tasks of varying complexity, ranging from state-to-state maps to full unitary maps in a large ($d = 16$) Hilbert space. We study the efficacy of numerical design and the performance of the resulting Hamiltonians, using as our test bed the electron and nuclear spins of individual ^{133}Cs atoms driven by radio frequency

(rf) and microwave (μw) magnetic fields [12,13]. Our experiments show that the optimal control strategy is adaptable to a wide range of tasks, and that it can generate control Hamiltonians with excellent performance in the presence of static and dynamic perturbations. On average, for large samples of randomly chosen transformations, we achieve fidelities from 0.982(2) for unitary maps to 0.995(1) for state maps (errors are one standard deviation). These results represent a significant advance in control complexity and fidelity compared to our prior work on state-to-state maps [13], and to state-of-the art for other systems with similar-sized Hilbert spaces [11,14]. Furthermore, given that the optimal control paradigm applies to any physical platform regardless of specifics, our work provides a useful template for similar advances elsewhere. Potential applications include improved fault tolerance in quantum computation [15–17], state preparation for quantum metrology [18], implementation of quantum simulations [19], and fundamental studies of open quantum systems and quantum chaos [20].

Introductions to optimal control can be found in the literature [2]. In the general case, one starts with a control Hamiltonian $H_C(t) = H_0 + \sum_j b_j(t)H_j$, chosen so it can generate all possible unitary maps and renders the system "controllable." The control waveforms are coarse grained in time, $\{b_j(t)\} \rightarrow \{b_j(t_k)\}$, to yield a discrete set of control variables. Given a target unitary W acting in the system space $\mathcal{H}$, one can search for a set $\{b_j(t_k)\}$ that minimizes the Hilbert-Schmidt distance $\|W - U(T)\|$, where $U(T)$ is the propagator driven by $H_C(t)$ during the time T. If the overall phase of W is unimportant, one can instead maximize the "standard" fidelity $\mathcal{F}_S = |\text{Tr}[W^\dagger U(T)]|^2/d^2$.

Similarly, a map W_{if} from an initial subspace $\mathcal{H}_i$ to a final subspace $\mathcal{H}_f$ can be obtained by maximizing $\mathcal{F}_S = |\text{Tr}[W_{if}^\dagger P_f U(T) P_i]|^2 / p^2$, where p is the dimension of, and P_i, P_f projectors onto, the subspaces. For a state map ($p = 1$) this reduces to $\mathcal{F}_S = |\langle \psi_f | U(T) | \psi_i \rangle|^2$. In practice $H_C(t)$ may depend on additional parameters $\Lambda = \{\lambda_i\}$ that are imperfectly known. If so, one can search for robust control waveforms by maximizing the average fidelity $\bar{\mathcal{F}}_S = \int_\Lambda \mathcal{P}(\Lambda) \mathcal{F}(\Lambda) d\Lambda$, where $\mathcal{P}(\Lambda)$ is the probability that the parameters take on the values Λ, and $\mathcal{F}(\Lambda)$ is the corresponding fidelity. If the parameters vary with time, one can average over an ensemble of histories, $\Lambda = \{\lambda_i(t)\}$, and search for control waveforms with built-in dynamical decoupling [21]. Robust control is essential in real-world scenarios, but until now little has been known about its feasibility in large Hilbert spaces.

The structure of the $6S_{1/2}$ electronic ground state of ^{133}Cs follows from the addition of electron and nuclear spins. The resulting Hilbert space has two manifolds with quantum numbers $F^{(\pm)} = I \pm S = 7/2 \pm 1/2 = 3, 4$, and overall dimension $d = 16$. As shown in [12], this system is controllable with a static bias magnetic field along z, a pair of phase-modulated rf magnetic fields along x and y, and a phase-modulated μw magnetic field coupling states $|F^{(\pm)}, m = F^{(\pm)}\rangle$. In the rotating wave approximation, the control Hamiltonian has the form

$$H_C(t) = H_0 + H_{\text{rf}}^{(+)}[\phi_x(t), \phi_y(t)] + H_{\text{rf}}^{(-)}[\phi_x(t), \phi_y(t)]$$
$$+ H_{\mu\text{w}}[\phi_{\mu\text{w}}(t)]. \tag{1}$$

Here H_0 is a drift term including the hyperfine interaction and Zeeman shift from the bias field, the $H_{\text{rf}}^{(\pm)}$ generate $SU(2)$ rotations of the $F^{(\pm)}$ hyperfine spins depending on the rf phases, and $H_{\mu\text{w}}$ generates $SU(2)$ rotations of the $|F^{(\pm)}, m = F^{(\pm)}\rangle$ pseudospin depending on the μw phases. Besides the control phases, $H_C(t)$ depends on the following parameters (nominal values in parenthesis): the Larmor frequency in the bias field ($\Omega_0 = 2\pi \times 1$ MHz), the rf Larmor frequencies in the rotating frame ($\Omega_x = \Omega_y = 2\pi \times 25$ kHz), the μw Rabi frequency ($\Omega_{\mu\text{w}} = 27.5$ kHz), and the rf and μw detunings from resonance ($\Delta_{\text{rf}} = \Delta_{\mu\text{w}} = 0$). For details see [22] and the accompanying supplemental material [23].

Following the general approach, we use control waveforms $\{\phi_x(t_k), \phi_y(t_k), \phi_{\mu\text{w}}(t_k)\}$ that correspond to piecewise constant phase modulation. Given some target unitary W, we start by choosing an overall control time T and phase-step duration δt, and then generate a random guess for the control phases. This seeds a gradient ascent algorithm, which eventually converges on a waveform corresponding to a local maximum of the fidelity. At each iteration $U(T)$ is found by integrating the Schrödinger equation, and the fidelity relative to W is computed.

When searching for robust control waveforms, we have found that our dominant source of uncertainty is spatial inhomogeneity of the bias field, and that maximizing a two-point average $\bar{\mathcal{F}}_S = [\mathcal{F}_S(B_0 + \delta B) + \mathcal{F}_S(B_0 - \delta B)]/2$ is sufficient for good performance. A similar approach might suffice for robust control of many other well-behaved physical systems. In more challenging scenarios, our experiments on state maps [13] and our numerical exploration of waveform design for more complex tasks show that robust control can be extended to additional inhomogeneous parameters. One can also compensate for larger inhomogeneous bandwidths than done here. In our case $\delta\Omega_0 = g_F \mu_B \delta B / \hbar$ is well below the frequency resolution $\sim 1/T$ of our waveforms, but robustness can be achieved across a significant fraction of the waveform modulation bandwidth $1/\delta t$ if the fidelity is maximized on a wider grid. As is generally the case, additional robustness requires more phase steps and longer control time. In practice most systems will have an upper limit on T, beyond which added robustness to inhomogeneous parameters is overwhelmed by other errors. In that case one is faced with a tradeoff involving the number of parameters and bandwidths for which robust control can be achieved.

In principle one can use standard optimization tools to search for control waveforms. We find it advantageous to supplement these with a modified version [24] of the numerically efficient GRAPE algorithm for the calculation of gradients [25]. With this we find optimization of individual waveforms to be straightforward on a desktop computer, and the design of large numbers of waveforms to be feasible on a high-performance cluster [26]. For appropriate T and δt a modest number of initial guesses (~ 10) typically lead to at least one waveform with theoretical fidelity ≥ 0.999. This is consistent with the benign character of control landscapes found in theoretical studies [27,28].

As expected, different quantum maps require control waveforms of different complexity. Figure 1(a) shows a robust waveform designed for a randomly chosen unitary map on the 16-dimensional Hilbert space $\mathcal{H}$. In this case every element of the matrices $U(T)$ and W must be identical. A d-dimensional unitary matrix W in $SU(d)$ requires $d^2 - 1$ real numbers to specify, and thus the waveforms must contain at least that many independent phases. In practice a substantially larger number is needed to achieve robust control. Similarly, Figs. 1(b) and 1(c) show waveforms for a unitary map on the 9-dimensional subspace of the $F^{(+)}$ manifold, and for a state-to-state map. These examples illustrate how control waveforms can be simpler and shorter as the constraints on $U(T)$ are relaxed.

Technical aspects of our laboratory setup were described in [13]. The basic experimental sequence is performed in parallel on $\sim 10^6$ laser cooled Cs atoms, and consists of initial state preparation, implementation of a quantum map, and a measurement of the output populations in the
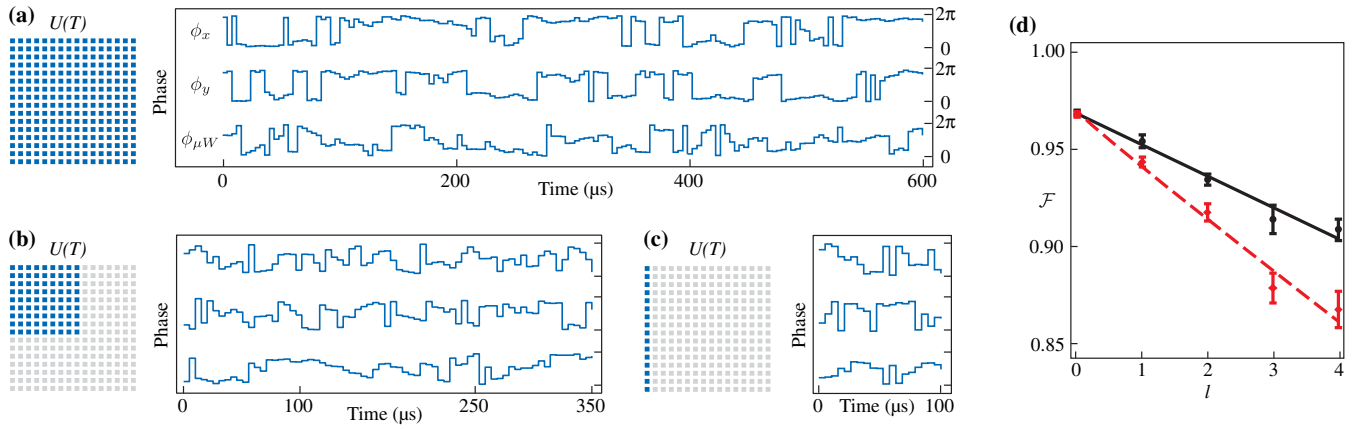
FIG. 1 (color online). Examples of phase modulation waveforms for different control tasks. (a) For a unitary map on $\mathcal{H}$ every element of $U(T)$ is constrained and the control waveforms must have at least $d^2 - 1 = 255$ independent phases. In our setup the optimal control time and phase step duration correspond to a total of 450 phases. (b) A unitary map on the $p = 9$ dimensional $F^{(+)}$ manifold constrains a $p \times p$ block of $U(T)$. The waveforms must contain at least $p^2 - 1 = 80$ phases, and we have successfully used a total of 210. (c) A state-to-state map in $\mathcal{H}$ constrains a single column of $U(T)$. The waveforms must contain at least $2d - 2 = 30$ phases, and we have successfully used a total of 60. (d) Randomized benchmarking data showing overall input-output fidelities for sequences of l unitary maps on $\mathcal{H}$, implemented with robust waveforms of the type shown in (a) (circles), or with nonrobust waveforms (diamonds). Each point represents an average of 10 sequences; error bars are $\pm$ one standard deviation of the mean. Lines are fits from which the benchmark fidelity $\mathcal{F}_B$ is determined.

magnetic sublevels $|F, m\rangle$. In principle one can reconstruct a quantum map through process tomography, but in practice this procedure is too error prone for our needs here. We rely instead on randomized benchmarking, a protocol originally developed for qubits [29], applied to state-to-state maps in [13], and here extended to general maps $\mathcal{H}_i \to \mathcal{H}_f$. The idea is to start with a random input state, apply a random sequence of l maps, and estimate its overall fidelity by measuring the population of the expected output state. This basic step is repeated many times for different l. Fitting the decay of the overall fidelity as a function of l then yields an accurate measure of the average fidelity per map.

An example of benchmarking data for a random sample of unitary maps on $\mathcal{H}$ is shown in Fig. 1(d), from which we estimate "benchmark" fidelities $\mathcal{F}_B = 0.982(2)$ and $\mathcal{F}_B = 0.971(1)$ for robust and nonrobust control waveforms. Similar data yield fidelities $\mathcal{F}_B = 0.984(2)$ for unitary maps on the $F^{(+)}$ subspace, $\mathcal{F}_B = 0.995(1)$ for maps between randomly chosen 2-dimensional subspaces $\mathcal{H}_i$, $\mathcal{H}_f$, and $\mathcal{F}_B = 0.995(1)$ for state maps, in all cases using robust waveforms. Note that the measured $\mathcal{F}_B$ lie consistently below our design goal of ≥ 0.999, the more so for complex tasks requiring longer waveforms. This is consistent with errors from experimental imperfections and external perturbations that accumulate over time.

The unitary maps of Fig. 1(d) were implemented with a control time and phase step duration identified as near-optimal based on computer-numerical and laboratory exploration [30]. Figure 2 shows the average fidelity calculated for that set of maps when implemented with

waveforms using a range of $(T, \delta t)$. Also shown are benchmark fidelities measured at a few discrete points. The primary feature is a high fidelity plateau, dropping sharply when T is too short for the required dynamical evolution, or the ratio $T/\delta t$ does not allow for a sufficient number of control phases. In our experiment the time scales for $T_{\min}$ and $\delta t_{\min}$ are set by the rf Larmor and μw Rabi frequencies, and for $\delta t_{\min}$ also by the rf modulation
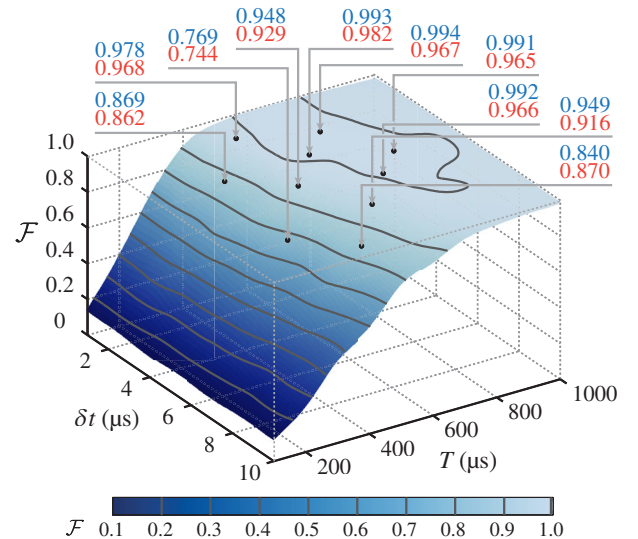

FIG. 2 (color online). Average fidelity $\mathcal{F}_S$ reached by a random set of unitary maps on $\mathcal{H}$, as function of the control time T and phase step duration δt. Numbers indicate average fidelities $\mathcal{F}_S$ (blue) and benchmarked fidelities $\mathcal{F}_B$ (red) for a few combinations T, δt. The top contour line is at $\mathcal{F}_S = 0.99$.

bandwidth. Less dramatically, the figure shows a small decline in fidelity for $T \gg T_{min}$ due to accumulating errors from imperfections and perturbations. Based on Fig. 2, the optimum combination is around $T = 600 \ \mu s$ and $\delta t = 4 \ \mu s$. Similar analyses show decreasing T_{min} for simpler tasks; we find optimal control times of $350 \ \mu s$ for unitary maps on the $F^{(+)}$ subspace, $180 \ \mu s$ for 2-dimensional maps $\mathcal{H}_i \rightarrow \mathcal{H}_f$, and $100 \ \mu s$ for state maps.

So far the focus has been on optimization for a given physical system and laboratory setup with its inherent imperfections and perturbations. To learn more about the prospects for control in less benign environments, we study the performance of robust control waveforms in the presence of larger, deliberately introduced perturbations. As an example, consider static and dynamic variations in the bias field, $B(t) = B_0 + \delta B(t)$. In our case $\delta B(t)$ is dominated by the 60 Hz power line cycle, and thus any change during control times $T \leq 1 \ ms$ will be approximately linear. This situation is typical of many cold-atom experiments, and might serve as a starting point for robust control of other well-behaved systems also. More complex time variations may be better characterized by frequency content, as in the design of advanced decoupling schemes for qubits [31].

Figure 3 shows predicted fidelities for unitary maps in the presence of perturbations $\delta B(t) = \delta B_i + (\delta B_f - \delta B_i)t/T$, characterized by the initial and final values of the bias field. Nonrobust waveforms were designed to maximize the fidelity at the nominal bias field, resulting in poor performance for even small δB_i, δB_f. Robust waveforms, by contrast, were designed to maximize the average fidelity for four different situations: two static offsets, $\delta B_i = \delta B_f$, and two linear variations, $\delta B_i = -\delta B_f$. This improves the fidelity significantly, expanding the 0.99 contour by a factor of 5 compared to nonrobust waveforms. Numerical modeling indicates these robust waveforms are also less sensitive to higher frequency, piece wise linear variations in the bias field. The tradeoff is a control time $T = 800 \ \mu s$, about 35% longer than for nonrobust waveforms.

To verify the performance of robust and nonrobust waveforms in the laboratory, we performed randomized benchmarking at points along the $\delta B_i = \delta B_f$ and $\delta B_i = -\delta B_f$ diagonals. As shown in Figs. 3(e) and 3(f), the predicted and observed increases in robustness agree reasonably well. Note also that in the absence of a deliberately applied perturbation, the robust waveforms achieve similar fidelity as Fig. 1(d), indicating that inherent dynamic perturbations are insignificant in our setup.

Looking ahead, one immediate issue is how to increase fidelity in our setup, whether by improving the accuracy of our control fields or further reducing external perturbations. It will also be advantageous to shorten control times, by increasing the strength and modulation bandwidth of our control fields, and/or by adding a second μw field to couple
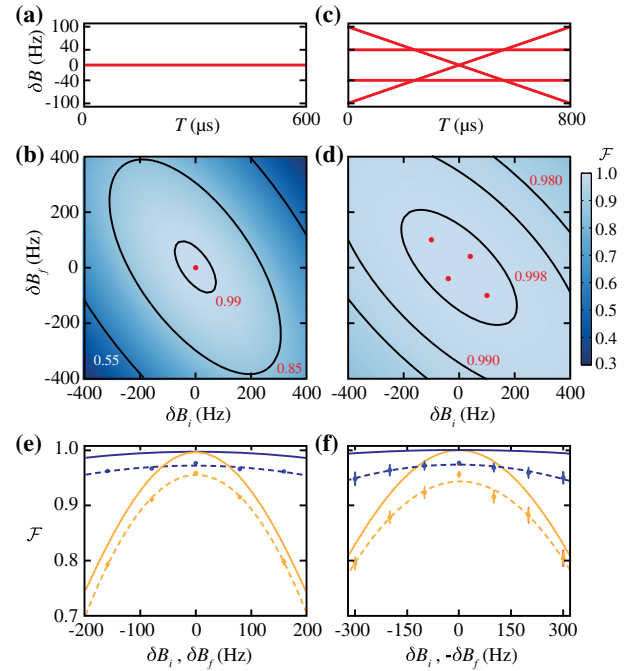

FIG. 3 (color online). Fidelity of robust vs nonrobust control waveforms for unitary maps on $\mathcal{H}$. (a) Bias field variation $\delta B(t)$ assumed in the design of nonrobust waveforms. (b) Average fidelity $\mathcal{F}_S$ predicted for these nonrobust waveforms when the actual $\delta B(t)$ changes linearly from δB_i to δB_f. The central dot corresponds to the variation in (a). (c) Bias field variations $\delta B(t)$ used for the four-point average that goes into the design of robust control waveforms. (d) Average fidelity $\mathcal{F}_S$ predicted for these robust waveforms as function of the actual δB_i, δB_f. Dots correspond to the variations in (c). (e) Measured and predicted fidelities for robust (blue) and nonrobust (orange) control waveforms, along the diagonal $\delta B_i = \delta B_f$. (f) Same along the diagonal $\delta B_i = -\delta B_f$. Data points in (e) and (f) show the average $\mathcal{F}_B$ for the set of maps; error bars are $\pm$ one standard deviation of the average. Dashed lines are parabolic fits to guide the eye. Solid lines show the predicted $\mathcal{F}_S$. Magnetic fields are given in units of Larmor frequency.

the states $|F^{(\pm)}, m = -F^{(\pm)}\rangle$. In the longer term there are a number of important questions to explore. What are the practical limits on optimal control, and will this permit accurate and robust control of less ideal systems? How large a Hilbert space is it realistic to control by the means used here? And how do the answers to these questions depend on the structure of the control Hamiltonian, notably its connectedness [28]? Can inhomogeneous control [32] be extended to qudits, perhaps allowing addressable unitary maps on large arrays [33]? And finally, is it possible to optimize control in the presence of decoherence [34], and perhaps extend it to (nonunitary) completely positive maps [35]? Some of these questions can be explored in our current system, while others await the application of optimal control to scalable architectures of interacting qubits and qudits.

———————

[1] L. M. K. Vandersypen and I. L. Chuang, Rev. Mod. Phys. **76**, 1037 (2005).

[2] C. Brif, R. Chakrabarti, and H. Rabitz, New J. Phys. **12**, 075008 (2010).

[3] M. Khasin and R. Kosloff, Phys. Rev. Lett. **106**, 123002 (2011).

[4] B. E. Mischuck, S. T. Merkel, and I. H. Deutsch, Phys. Rev. A **85**, 022302 (2012).

[5] M. M. Müller, D. M. Reich, M. Murphy, H. Yuan, J. Vala, K. B. Whaley, T. Calarco, and C. P. Koch, Phys. Rev. A **84**, 042315 (2011).

[6] R. Bartels, S. Backus, E. Zeek, L. Misoguti, G. Vdovin, I. P. Christov, M. M. Murnane, and H. C. Kapteyn, Nature (London) **406**, 164 (2000).

[7] S. Chaudhury, S. Merkel, T. Herr, A. Silberfarb, I. H. Deutsch, and P. S. Jessen, Phys. Rev. Lett. **99**, 163002 (2007).

[8] G. De Chiara, T. Calarco, M. Anderlini, S. Montangero, P. J. Lee, B. L. Brown, W. D. Phillips, and J. V. Porto, Phys. Rev. A **77**, 052333 (2008).

[9] F. Caruso, S. Montangero, T. Calarco, S. F. Huelga, and M. B. Plenio, Phys. Rev. **85**, 042331 (2012).

[10] F. Dolde, V. Bergholm, Y. Wang, I. Jakobi, B. Naydenov, S. Pezzagna, J. Meijer, F. Jelezco, P. Neumann, T. Schulte-Herrbrüggen, J. Biamonte, and J. Wrachtrup, Nat. Commun. **5**, 3371 (2014).

[11] R. Barends, J. Kelly, A. Megrant, A. Veitia, D. Sank, E. Jeffrey, T. C. White, J. Mutus, A. G. Fowler, B. Campbell, Y. Chen, Z. Chen, B. Chiaro, A. Dunsworth, C. Neill, P. O'Malley, P. Roushan, A. Vainsencher, J. Wenner, A. N. Korotkov, A. N. Cleland, and J. M. Martinis, Nature (London) **508**, 500 (2014).

[12] S. T. Merkel, P. S. Jessen, and I. H. Deutsch, Phys. Rev. A **78**, 023404 (2008).

[13] A. Smith, B. E. Anderson, H. Sosa-Martinez, C. A. Riofrío, I. H. Deutsch, and P. S. Jessen, Phys. Rev. Lett. **111**, 170502 (2013).

[14] T. Monz, P. Schindler, J. T. Barreiro, M. Chwalla, D. Nigg, W. A. Coish, M. Harlander, W. Hänsel, M. Hennrich, and R. Blatt, Phys. Rev. Lett. **106**, 130506 (2011).

[15] E. T. Campbell, Phys. Rev. Lett. **113**, 230501 (2014).

[16] F. H. E. Watson, E. T. Campbell, H. Anwar, and D. E. Browne, arXiv:1503.08800.

[17] S. Muralidharan, C.-L. Zou, L. Li, J. Wen, and L. Jiang, arXiv:1504.08054.

[18] V. Giovannetti, S. Lloyd, and L. Maccone, Nat. Photonics **5**, 222 (2011).

[19] P. Doria, T. Calarco, and S. Montangero, Phys. Rev. Lett. **106**, 190501 (2011).

[20] S. Chaudhury, A. Smith, B. E. Anderson, S. Ghose, and P. S. Jessen, Nature (London) **461**, 768 (2009).

[21] L. Viola, E. Knill, and S. Lloyd, Phys. Rev. Lett. **82**, 2417 (1999).

[22] C. A. Riofrío, P. S. Jessen, and I. H. Deutsch, J. Phys. B **44**, 154007 (2011).

[23] See Supplemental Material at http://link.aps.org/supplemental/10.1103/PhysRevLett.114.240401 for the detailed form of our control Hamiltonian.

[24] F. Motzoi, J. M. Gambetta, S. T. Merkel, and F. K. Wilhelm, Phys. Rev. A **84**, 022307 (2011).

[25] N. Khaneja, T. Reiss, C. Kehlet, T. Schulte-Herrbrüggen, and S. J. Glaser, J. Magn. Reson. **172**, 296 (2005).

[26] B. E. Anderson, Ph.D. thesis, University of Arizona, 2013, http://arizona.openrepository.com/arizona/handle/10150/305872.

[27] H. A. Rabitz, M. M. Hsieh, and C. M. Rosenthal, Science **303**, 1998 (2004).

[28] K. W. Moore, R. Chakrabarti, G. Riviello, and H. Rabitz, Phys. Rev. A **83**, 012326 (2011).

[29] E. Knill, D. Leibfried, R. Reichle, J. Britton, R. B. Blakestad, J. D. Jost, C. Langer, R. Ozeri, S. Seidelin, and D. J. Wineland, Phys. Rev. A **77**, 012307 (2008).

[30] K. W. Moore Tibbetts, C. Brif, M. D. Grace, A. Donovan, D. L. Hocker, T. S. Ho, R. B. Wu, and H. Rabitz, Phys. Rev. A **86**, 062309 (2012).

[31] M. J. Biercuk, H. Uys, A. P. VanDevender, N. Shiga, W. Itano, and J. J. Bollinger, Nature (London) **458**, 996 (2009).

[32] K. Kobzar, B. Luy, N. Khaneja, and S. J. Glaser, J. Magn. Reson. **173**, 229 (2005).

[33] J. H. Lee, E. Montano, I. H. Deutsch, and P. S. Jessen, Nat. Commun. **4**, 2027 (2013).

[34] N. Khaneja, T. Reiss, B. Luy, and S. J. Glaser, J. Magn. Reson. **162**, 311 (2003).

[35] R. Wu, A. Pechen, C. Brif, and H. Rabitz, J. Phys. A **40**, 5681 (2007).